



# Microstructural Stability of Al<sub>3</sub>Si<sub>2.5</sub>Cu Alloy in the Semisolid State Produced via Deformation via Equal Channel Angular Pressing (ECAP)

Luis Vanderlei Torres<sup>1</sup> · Bruna Vilas Bôas<sup>2</sup> · João Paulo de Oliveira Paschoal<sup>3</sup> · Eugênio José Zoqui<sup>3</sup>

Received: 14 February 2024 / Revised: 14 May 2024 / Accepted: 22 May 2024  
© ASM International 2024

## Abstract

This work aims to evaluate the thixoformability of the Al–Si–Cu alloy regarding microstructural evolution during its reheating at semisolid temperature. Low-silicon aluminum alloys are not used in casting processes but can be a viable alternative for processing in the semisolid state. In this attempt, the Al–3wt%Si–wt%2.5Cu alloy was tested. The material was produced via direct casting and then submitted to equal channel angular pressing (ECAP)—single pass. After that, for two conditions of solid fractions, 45% and 60%, globularization heat treatments were carried out for 0, 30, and 90 s. Grain size of 108 μm, globule size of 47 μm, and circularity of 0.62 were achieved, showing microstructure refinement. This demonstrates that using the ECAP process becomes an effective tool in the globularization of the microstructure and, thus, the thixoforming process. As thermodynamic and microstructural stability guarantee reasonable viscosity control and good processing control, the raw material production route via ECAP can be an excellent solution for thixoforming processes, especially for these alloys with low Silicon content.

**Keywords** Semisolid material · Thixoforming · ECAP · Al–Si–Cu alloy · Microstructure

## Introduction

Semisolid technology emerged in the 1970s at the Massachusetts Institute of Technology (MIT) during the development of doctoral research on shrinkage cracks in the Sn–15wt%Pb alloy, where it was found that the intense agitation of the casting metal during solidification considerably affected the dendritic morphology, leading to the breakage of its arms; the dendritic arms of the microstructure when in the semisolid state are transformed

into globules or a structure of primary phase close to spherical [1]. This technology has several advantages over conventional casting: greater energy efficiency, productivity, lower porosity, longer mold life due to less thermal shock, and fine and uniform microstructures with improved properties. Furthermore, what stands out the most is the possibility of producing parts in the near-net-shape condition; that is, the part is formed practically in the final shape of the product, eliminating machining steps, reducing the loss of material and, consequently, reducing the final cost of production [2].

In the 1990s, the development of automotive products began using semisolid technology from aluminum alloys [3]; what triggered this development was the oil crisis between the 1970s and 1980s, which sought lighter materials to reduce the weight of vehicles [4–6]. This development of products manufactured using semisolid technology made the automotive industry the leading destination for these products, comprising suspension systems, housings, clutch disks, etc. [7, 8]. Some regions stand out regarding the application of this technology, such as Europe, which produces products for the automotive sector; the USA, which makes parts for bicycles and snowmobiles; and Asia, which produces electronic components in magnesium alloys. [2].

This invited article is part of a special topical focus in the journal *Metallography, Microstructure, and Analysis* on Quantitative Metallography and Microstructure Modeling.

✉ Luis Vanderlei Torres  
torres@ifsp.edu.br

<sup>1</sup> Federal Institute of Education, Science and Technology of São Paulo - IFSP, Bragança Paulista, SP 12903-000, Brazil

<sup>2</sup> Federal Institute of Education, Science, and Technology of São Paulo - IFSP, Sorocaba, SP 18095-410, Brazil

<sup>3</sup> Materials and Manufacturing Department, Faculty of Mechanical Engineering, University of Campinas, UNICAMP, Campinas, SP 13083-860, Brazil

Deformation via ECAP emerged between the 1980s and 1990s and is known as one of the most interesting and commonly used methods to impose large deformations and produce microstructural refinement in metallic materials. In this process, the sample was pressed against a die with channels of the same cross-section that meet at an angle  $\Phi$ , normally  $90^\circ$  or  $120^\circ$ . This configuration of channels causes the material that passes through them to be deformed by simple shear without its cross-section being significantly altered [9]. Most published work on this topic involves using magnesium alloys [10, 11]. Ashouri et al. [12] were the first to publish work using the ECAP process to produce thixotropic raw material using the A356 aluminum alloy. Currently, the spherical morphology can be obtained through several processing routes, and one of them involves the thermomechanical treatment of the raw material, in which the alloy used is deformed and then reheated to a semisolid state. Deformation can be done by rolling, forging, and extrusion; however, the homogeneity and intensity of deformation induced by each pass are limited, stimulating the development and application of new processes [12, 13].

Thus, searching for processes that facilitate the obtainment of globular morphology has been one of the main subjects in the semisolid field in recent years. In this sense, the present study aims to contribute to developing the use of deformation via ECAP in producing semisolid raw materials. As a specific objective, the evaluation of the microstructural evolution of the semisolid Al–3wt%Si–wt%2.5Cu, or simply Al3Si2.5Cu, alloy made via the ECAP process through different processing parameters, such as semisolid temperature and waiting time during globularization heat treatment, is a specific objective.

## Materials and Methods

The alloy under study was melted in a resistive furnace at a temperature of  $750^\circ\text{C}$  (higher than its melting point) in pre-insulated silicon carbide crucibles with QF180 (silico-aluminous) using a mixture of base alloys: alloy A356, commercially pure aluminum (Al-cp), commercially pure copper (Cu-cp) and grain-refining alloy Al–5wt%Ti–1wt%B, and then, it was poured into an electromagnetic stirring system with approximately 8 kW of power, generating a magnetic field of 13 Gauss; 5 kg of raw material was produced, about 12 ingots measuring 250 mm in length and 30 mm in diameter [14]. The chemical composition, presented in Table 1, was determined using a Bill OES model optical emission spectrometry system.

The characterization of the working temperatures, that is, the temperature interval between the solidus and liquidus lines, took place through DSC analysis (Differential Scanning Calorimetry) and via Thermo-Calc<sup>®</sup> software

**Table 1** Chemical composition of the Al3Si2.5Cu alloy obtained via optical emission spectrometry (wt%)

Si	Cu	Mg	Ti	Fe	Al
$3.00 \pm 0.06$	$2.54 \pm 0.11$	$0.12 \pm 0.05$	$0.15 \pm 0.03$	$0.13 \pm 0.07$	Bal.

simulations (TTAL5 database). The DSC tests were carried out in a NETZSCH thermal analysis equipment, model STA-409C, where samples with a mass of 100 mg were used and inserted into alumina crucibles to carry out the tests, using two heating rates ( $5^\circ\text{C}/\text{min}$  and  $20^\circ\text{C}/\text{min}$ ) to  $700^\circ\text{C}$  and cooling to room temperature with analogous cooling rate. In simulations via Thermo-Calc<sup>®</sup> software, the ideal composition of the alloy under study was used, therefore excluding any inclusions or residual elements; in these simulations, the software employed a calculation routine evaluating solidification conditions in and out of equilibrium based on the Lever Rule and Scheil models.

Figure 1a shows the liquid fraction versus temperature, and Fig. 1b shows the sensitivity of liquid formation versus temperature, obtained through DSC tests and Thermo-Calc<sup>®</sup> software simulations. Only the heating rates data were used since it is a thixoforming procedure rather than rheocasting. Figure 1a shows the partial melting of the eutectic at a relatively low temperature, forming about 15% liquid. The inflexion in the curve, at about  $562^\circ\text{C}$ , marks the beginning of the melting of the  $\text{Al}_\alpha$  primary phase. Thixoforming operation must occur after melting the eutectic. Liu et al. [15] proposed thermodynamic criteria to classify an alloy as a suitable raw material to be used in thixoforming processes, namely temperature range for complete solidification ( $\Delta T$ ) below  $130^\circ\text{C}$  and sensitivity ( $S = |\text{dlf}/\text{dT}| = |\text{dfs}/\text{dT}|$ ) be less than  $0.030^\circ\text{C}^{-1}$ . Figure 1b shows the variation in sensitivity as a function of temperature. In the eutectic melting region, there is an increase in sensitivity, demonstrating that the partial melting of the eutectic is unstable and, therefore, difficult to control. For higher temperatures and lower solid fractions, where the liquid coexists with the solid  $\text{Al}_\alpha$ , there is less sensitivity and more possibility of managing the process. Table 2 summarizes the temperatures and the corresponding sensitivity found; it is observed that, for all methods used, the sensitivity at the target temperatures was lower than the proposed maximum value for both solid fractions ( $600 \pm 2^\circ\text{C}$  for 45% and  $615 \pm 2^\circ\text{C}$  for 60% of the solid fraction). Thermo-Calc<sup>®</sup> software simulation showed the lowest values. Therefore, the material presents stability in the semisolid state and can be used in thixoforming processes.

The deformation via ECAP occurred through a metal matrix with cylindrical channels with cross sections of 30 mm and an angle of  $120^\circ$ . A hydraulic press with a capacity of 50 tons operating at a maximum speed of

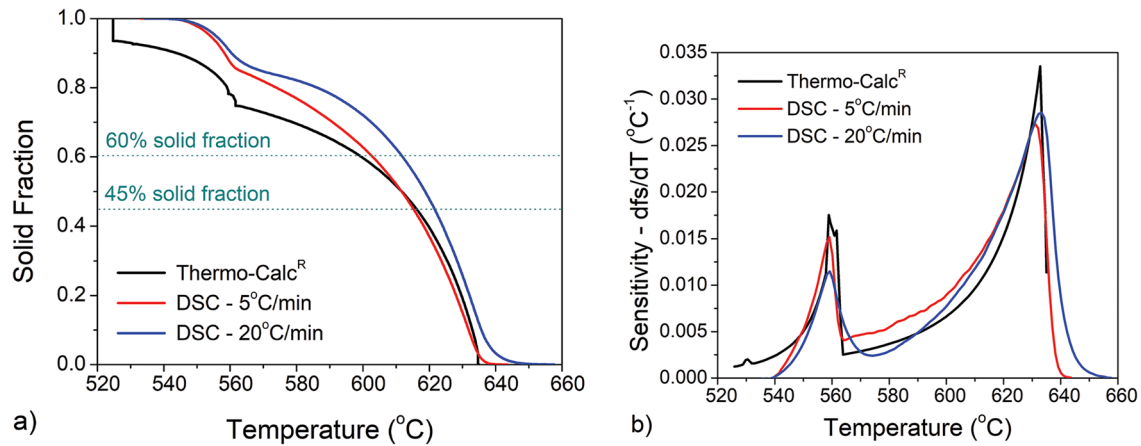


**Fig. 1** Solid fraction versus temperature (a) and the corresponding sensitivity (b), both obtained through DSC tests and via Thermo-Calc<sup>®</sup> software simulations

**Table 2** Summary of the temperatures found for the Al3Si2.5Cu alloy via DSC analysis and Thermo-Calc<sup>®</sup> software simulations

Technique	T solidus (°C)	T liquidus (°C)	ΔT (°C)	T 45% fs/dlff/dT (°C/°C <sup>-1</sup> )	T 60% fs/dlff/dT (°C/°C <sup>-1</sup> )
Thermo-Calc <sup>®</sup>	525	633	108	615/0.009	599/0.008
DSC - 5 °C/min	542	643	101	615/0.009	603/0.010
DSC - 20 °C/min	543	657	114	621/0.016	612/0.011

approximately 7 mm/s imposed a single pass through the die on ingots lubricated with MoS<sub>2</sub>. The 30-mm-diameter and 150-mm-long ingots were heated to 300 °C, enough to avoid superficial cracks but also to allow a better passage of the material through the matrix, which was also heated to a temperature of 100 °C to prevent heat loss during the process with the help of electrical resistances placed around it [16–18].

The temperatures found in the DSC tests and simulations via Thermo-Calc<sup>®</sup> software were tested in the heat treatment of globularization under the condition of a solid fraction of 45% to determine the best working temperatures; the temperatures indicated by the simulation via the Thermo-Calc<sup>®</sup> software were more consistent during the tests, being adopted as working temperatures for the test conditions stipulated in this work, because when the temperatures obtained through the DSC tests with the highest heating rate (20 °C/min) were adopted, the samples melted, causing its automatic exclusion [19]. Globularization heat treatments were carried out from samples of 25 mm in height and 30 mm in diameter for approximately 6 min in a Norax induction furnace (25 kW, 8 kHz) with a 100 °C/min heating rate. When the samples reached the temperatures corresponding to the solid fractions of 45% and 60%, i.e., 615 and 600 °C, they were kept at 0, 30, and 90 s and then cooled in water. The samples produced were characterized by optical

microscopy for microstructural evaluation via conventional and color metallography.

For the microstructural characterization, the samples were sectioned longitudinally, sanded with water sandpaper with a granulometry of 220, 320, 400, 600, 800, 1200, and 1500, and polished with diamond paste of 6 μm and 1 μm. After polishing, the samples were etched with HF reagent (1 ml and 99 ml H<sub>2</sub>O), the attack was performed with the total immersion of the sample in the reagent for a time of 10 s, and then, the samples were rinsed in running water for approximately 30 s and dried using an electric blower. For the microstructural characterization via color metallography, the samples used in the previous characterization underwent an electrolytic attack with the deposition of HBF<sub>4</sub> (fluoroboric acid) in a 2.0% solution and voltage of 25 V for approximately 6 min with moderate and constant agitation. A Leica DM ILM optical microscope was used to acquire the images, and polarizing filters were used to obtain the colored pictures, making grains with the same crystalline orientation present similar coloration, which makes their identification and respective characterization easier. For the measurements of the size of primary particles and grains, the Heyn Intercept Method, governed by the ASTM E112 standard, was used [20]. The count was performed in five different fields of each image, and for each sample, five images of various sections were used, totaling twenty-five counts of primary globules and grains. The form factor used in this

work was circularity, using the ImageJ 1.40 g software; the software tends to highlight the grain contours of the image and, based on the geometry of such contours, assigns a value that varies from 0 to 1 for each contour, with the value “1” being transferred to a perfectly circular contour, and as contour geometry deviates from this shape, a lower value is assigned to it. Finally, with the information on the sizes of primary globules and grains available, Zoqui [21] developed the rheocast quality index (RQI), which correlates microstructural parameters, thus allowing the analysis of the efficiency of the method of obtaining the raw material, and is given by:  $RQI = (\text{primary globule} \cdot \text{circularity}) / \text{grain size}$ .

Chemical composition analyses were also carried out using energy-dispersive x-ray spectroscopy (EDS) and scanning electron microscopy scanning electron microscopy (SEM) using a ZEISS EVO/MA15 microscope to identify the elements and phases present in the alloy (map with the chemical distribution and punctual aspects of the matrix and constituents); for this, the samples were prepared using the same procedure previously described for optical microscopy (sanding and polishing).

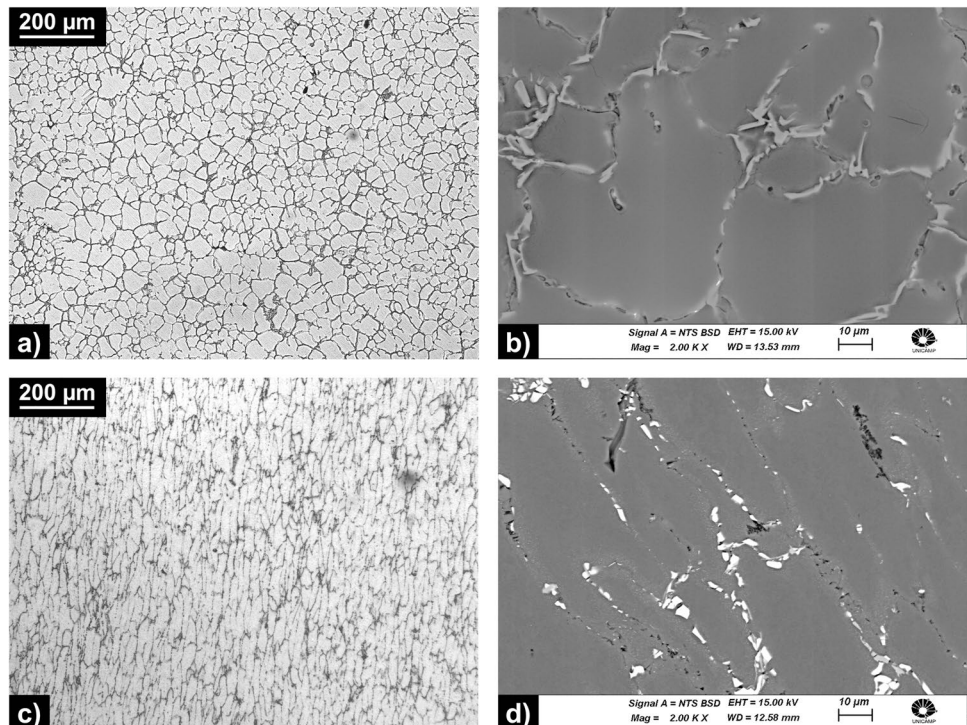
## Results and discussion

Figure 2 shows the alloy's microstructure under the as-casting and plastically deformed by the ECAP process conditions. It is observed in Fig. 2a that under the casting condition, a rosette-shaped morphology is presented

due to the use of the Al5Ti1B grain refining alloy and the electromagnetic stirring. These structures comprise the primary phase ( $\alpha$ -Al) with the eutectic phase (Al–Si) distributed in the grain boundary. Figure 2b shows the morphology of the Al–Si eutectic of the casting alloy via scanning electron microscopy (SEM), in which irregular Si particles with fibber-like morphology can be observed. For the condition via the ECAP process, Fig. 2c shows a structure with elongated grains taking place due to the deformation imposed by the process. However, the material recrystallizes when reheated, and new grains are formed. Figure 2d shows, via scanning electron microscopy (SEM), the morphology of the Al–Si eutectic of the deformed alloy. The elongated Si particles are fragmented due to the material passing through the extrusion die channel. Campo [22] observed the same morphological transformations in the A356 alloy processed via ECAP; the primary phase and the eutectic appear elongated in the direction of deformation, and the more elongated Si particles fragment with the imposed deformation.

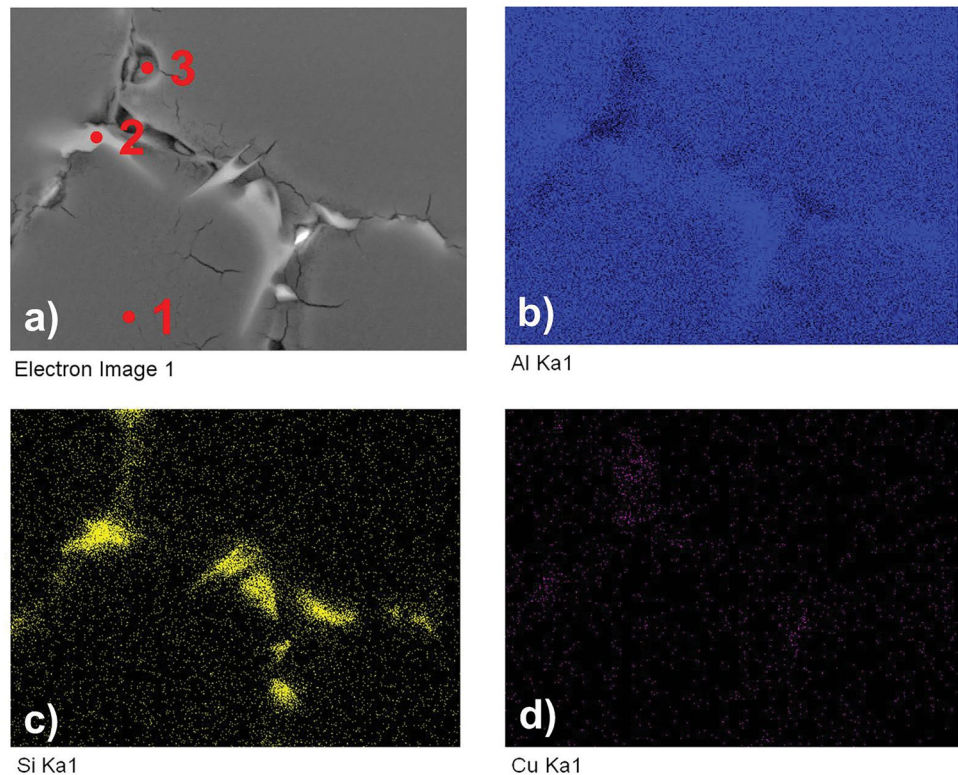
Figure 3 shows the microstructure and the matrix chemical composition for the initial casting condition via the RX-EDS map. The elements aluminum (Al), silicon (Si), and copper (Cu) in higher concentrations are highlighted, and a similar result is obtained in the analysis of the punctual chemical composition in the eutectic and intermetallic alloy phases. It can be observed that the Si and Cu elements are concentrated in the grain boundary. In contrast, the Mg, Fe, and Ti elements are uniformly distributed throughout

**Fig. 2** Microstructure of the Al3Si2.5Cu alloy: conventional metallography under the casting condition (a), eutectic morphology under the casting condition (b), traditional metallography under the plastically deformed condition by the ECAP process (c), and the plastically twisted condition by the process ECAP (d)





**Fig. 3** Micrograph via SEM of the Al3Si2.5Cu alloy at casting condition, showing the points used for the punctual chemical analysis: Al<sub>α</sub> matrix (point 1), Al–Si eutectic phase (point 2), and the intermetallic Al<sub>2</sub>Cu (point 3). RX-EDS map of the chemical composition for the elements Al (**b**), Si (**c**), Cu (**d**)



the material (not shown due to the low content). Figure 3a analyzes the punctual chemical composition of the present phases. The chemical composition of the matrix, measured at point 1, is composed of Al, containing low levels of silicon and copper, as shown in Table 3. The average composition of the eutectic, measured at point 2, is composed of a large amount of Si. At point 3, the intermetallic Al<sub>2</sub>Cu, composed of a large amount of Cu, can be verified.

Figure 4 presents the SEM microstructure, and the chemical composition of the matrix is observed via the RX-EDS map under the condition of being plastically deformed by the ECAP process. The elements aluminum (Al), silicon (Si), and copper (Cu) in higher concentrations are highlighted, as seen for the initial condition (casting) and like that obtained in the analysis of the punctual chemical composition in the eutectic and intermetallic phases of the alloy. It can be observed that the Si and Cu elements are concentrated in the grain boundary. In contrast, the Mg, Fe, and Ti elements are uniformly distributed throughout the material and not shown due to the low content. Figure 4a

analyzes the punctual chemical composition of the present phases. The chemical composition of the matrix, measured at point 1, is composed mainly of Al, containing low levels of silicon and copper, as shown in Table 4. The average composition of the eutectic, measured at point 2, is composed of a large amount of Si. Finally, in point 3, the presence of the intermetallic Al<sub>2</sub>Cu, composed of a large amount of Cu, is verified.

Figures 5 and 6 show the micrographs via conventional metallography and color metallography of the heat-treated alloy for the solid fractions of 45% and 60% at times of 0, 30, and 90 s produced by the ECAP process. The image analysis system using polarized light (color metallography) proved to be efficient for determining the grain size of the alloy since, according to metallurgical concepts, each grain differs from the other due to different crystallographic orientations. Therefore, under polarized light, different grains have different colors. Besides, it can be noted that the reheating to the semisolid state (solid fractions of 45% and 60%) was sufficient to promote efficient globularization of the solid

**Table 3** Point analysis by EDS of the Al<sub>3</sub>Si<sub>2.5</sub>Cu alloy under the casting condition (wt%)

Phases	Points	Elements (wt%)				
		Al	Si	Cu	Mg	Fe
Al	1	98.12	1.08	0.79	–	–
Si eutectic (Al–Si)	2	64.75	32.98	2.27	–	–
Al <sub>2</sub> Cu	3	64.83	2.30	32.87	–	–

**Fig. 4** Micrograph via SEM of the Al<sub>3</sub>Si<sub>2.5</sub>Cu alloy at plastically deformed by the ECAP process, showing the points used for the punctual chemical analysis: Al<sub>α</sub> matrix (point 1), Al–Si eutectic phase (point 2), and the intermetallic Al<sub>2</sub>Cu (point 3). RX-EDS map of the chemical composition for the elements Al (b), Si (c), Cu (d)

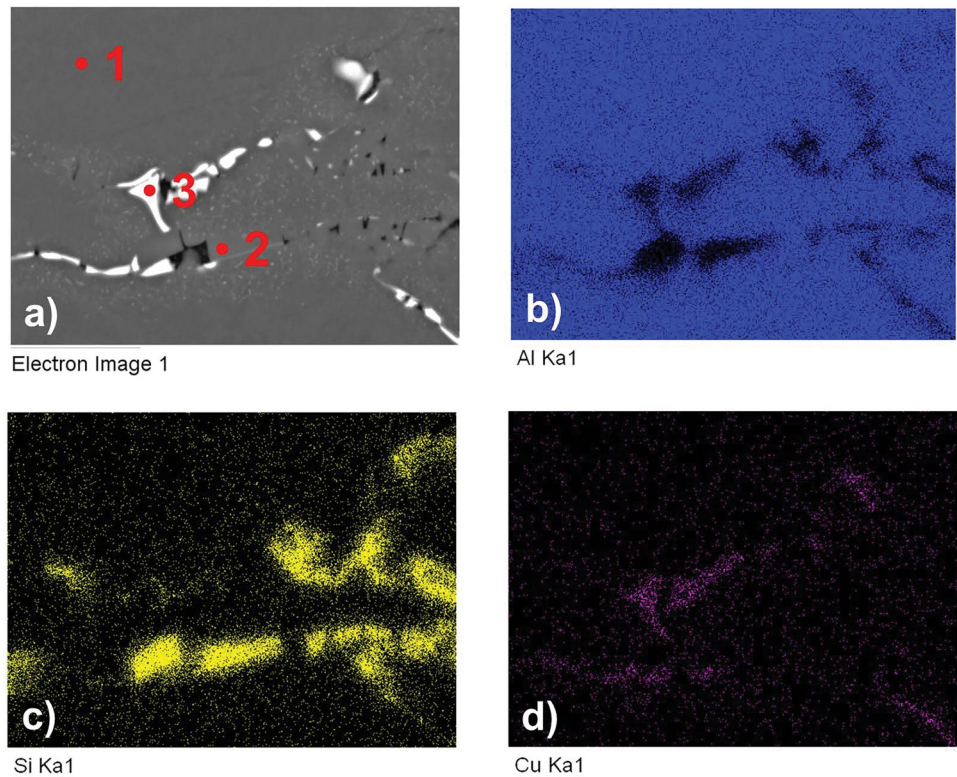


**Table 4** Point analysis by EDS of the Al<sub>3</sub>Si<sub>2.5</sub>Cu alloy under the condition plastically deformed by the ECAP process (wt%)

Phases	Points	Elements (wt%)				
		Al	Si	Cu	Mg	Fe
Al	1	97.49	0.87	1.63	–	–
Si eutectic (Al–Si)	2	76.55	20.37	3.09	–	–
Al <sub>2</sub> Cu	3	48.75	1.17	49.39	–	0.69

phase necessary for the thixoforming processes, even for the reheating time of 0 s, with no significant size variation of primary globules and grains.

In general, the microstructure obtained via conventional metallography (Fig. 5) presents small primary globules due to the recrystallization that occurred, which is the primary mechanism in the formation of spherical particles from grains deformed during reheating, determining the distribution and size of globules in the metallic slurry. Regardless of the waiting time, it is noted that a microstructure formed by primary globules is almost entirely spherical. The circularity indicates how much the structure is spherical (circular); thus, it is observed that there were no significant differences in its value with the increase in the waiting time for the different test conditions. Table 5 summarizes the metallurgical parameters analyzed in this study: the average size of primary globules and grains, roundness form factor, and RQI; the same results can be seen graphically in Figure 7.

Note that the effect of heating time is minimal in terms of changing the grain size of the globule and that there is no significant effect on its morphology. This is information of great importance for process control since the size and morphology of solid particles determine viscous behavior. In this way, there is an excellent confluence between information from thermodynamic analysis and morphological analysis. Mapping the solid-liquid transformation indicated that the material remains stable regarding the amount of solid fraction; the Al<sub>3</sub>Si<sub>2.5</sub>Cu alloy showed low sensitivity to temperatures of 600 and 615 °C. This first information, combined with the fact that the grain size, globule size, and shape factor change little when the material is kept at high temperature, indicates a material with high stability for processing. In other words, small temperature fluctuations and small time fluctuations during processing will have little effect on the rheology of the slurry, leading to a situation where processing is easily controllable.



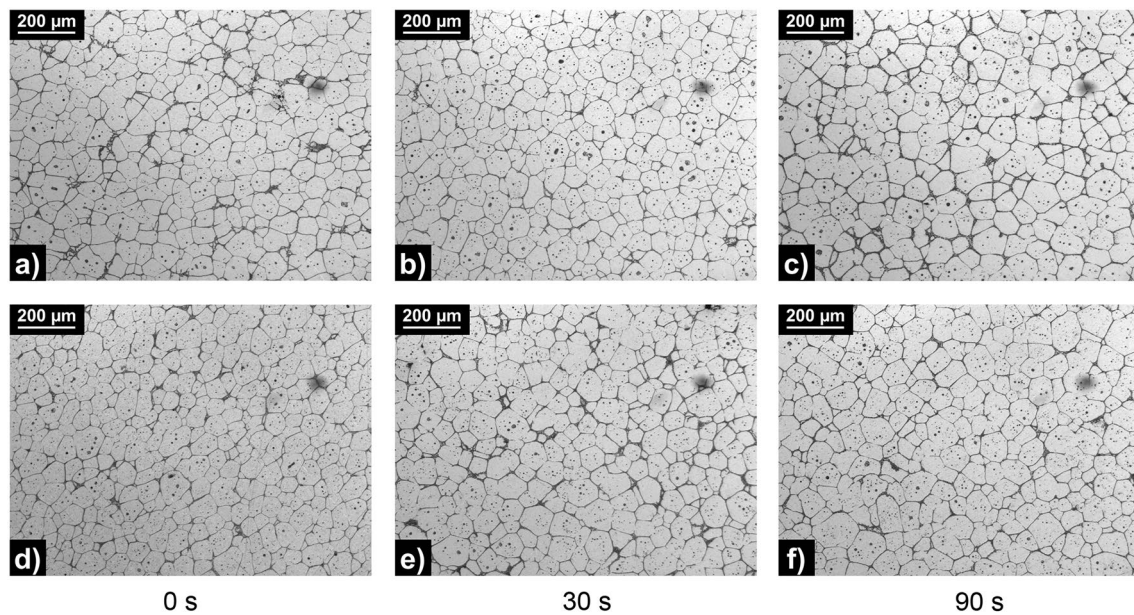


**Fig. 5** Conventional metallography of the heat-treated Al<sub>3</sub>Si<sub>2.5</sub>Cu alloy for the solid fractions of 45% (a–c) and 60% (d–f) at different treatment times

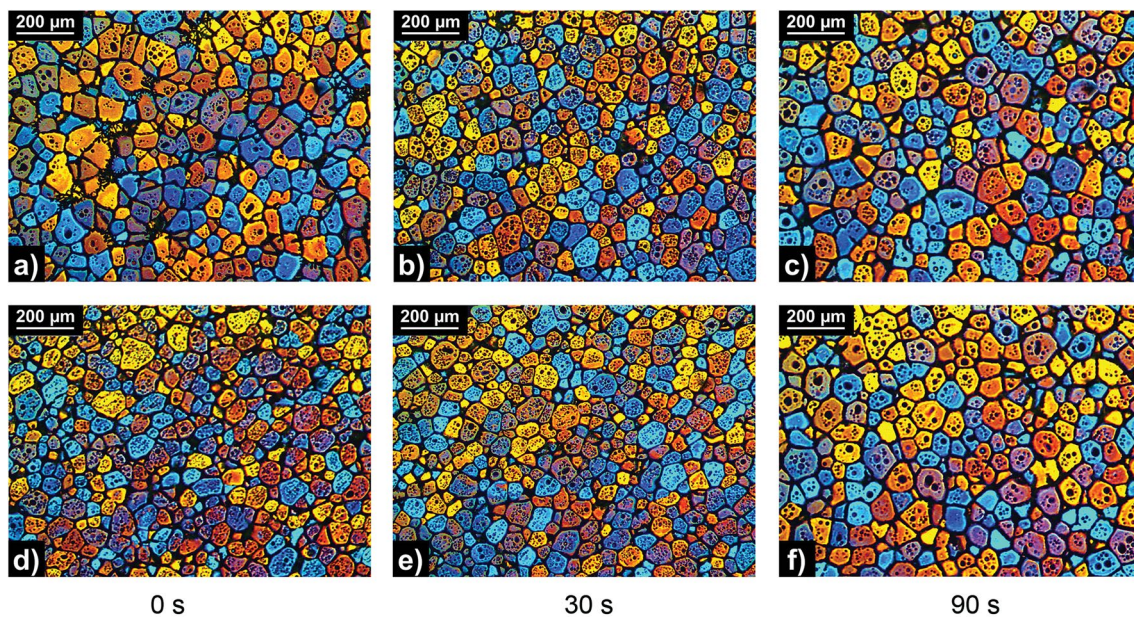


**Fig. 6** Color metallography of the heat-treated Al<sub>3</sub>Si<sub>2.5</sub>Cu alloy for the solid fractions of 45% (a–c) and 60% (d–f) at different treatment times

Torres et al. [18], when analyzing through microstructural analysis the Al<sub>4</sub>Si<sub>2.5</sub>Cu alloy produced by the ECAP process, found that the alloy showed an excellent response to the recovery and recrystallization mechanisms with an average primary globule size of 45  $\mu\text{m}$  and an average grain size of 75  $\mu\text{m}$ . Proni et al. [17] analyzing three Al–Si–Cu alloys (with a silicon content of 5 wt%, 6 wt%, and 7 wt%) produced by the ECAP process also obtained the same

results; that is, the alloys responded satisfactorily to the recovery phenomena and recrystallization and exhibited refined microstructures after reheating to a semisolid state without significant changes in size or shape, facts that collaborate with the study.

**Table 5** Summary of the metallurgical parameters analyzed for the Al<sub>3</sub>Si<sub>2.5</sub>Cu alloy—primary globule (GLS) and grain (GS) average size, circularity, and rheocast quality index (RQI)

Solid fraction (%)	Treatment time (s)	Primary globule ( $\mu\text{m}$ )	Circularity	Grain Size ( $\mu\text{m}$ )	RQI
45	As-cast	$34 \pm 3$	$0.43 \pm 0.13$	$65 \pm 11$	$0.20 \pm 0.07$
	0	$45 \pm 4$	$0.65 \pm 0.17$	$116 \pm 24$	$0.25 \pm 0.09$
	30	$48 \pm 6$	$0.64 \pm 0.17$	$105 \pm 31$	$0.29 \pm 0.09$
60	0	$46 \pm 5$	$0.66 \pm 0.18$	$127 \pm 16$	$0.24 \pm 0.11$
	30	$47 \pm 7$	$0.58 \pm 0.16$	$101 \pm 20$	$0.27 \pm 0.09$
	90	$44 \pm 5$	$0.62 \pm 0.14$	$94 \pm 09$	$0.29 \pm 0.07$
	90	$52 \pm 7$	$0.59 \pm 0.15$	$108 \pm 13$	$0.28 \pm 0.07$

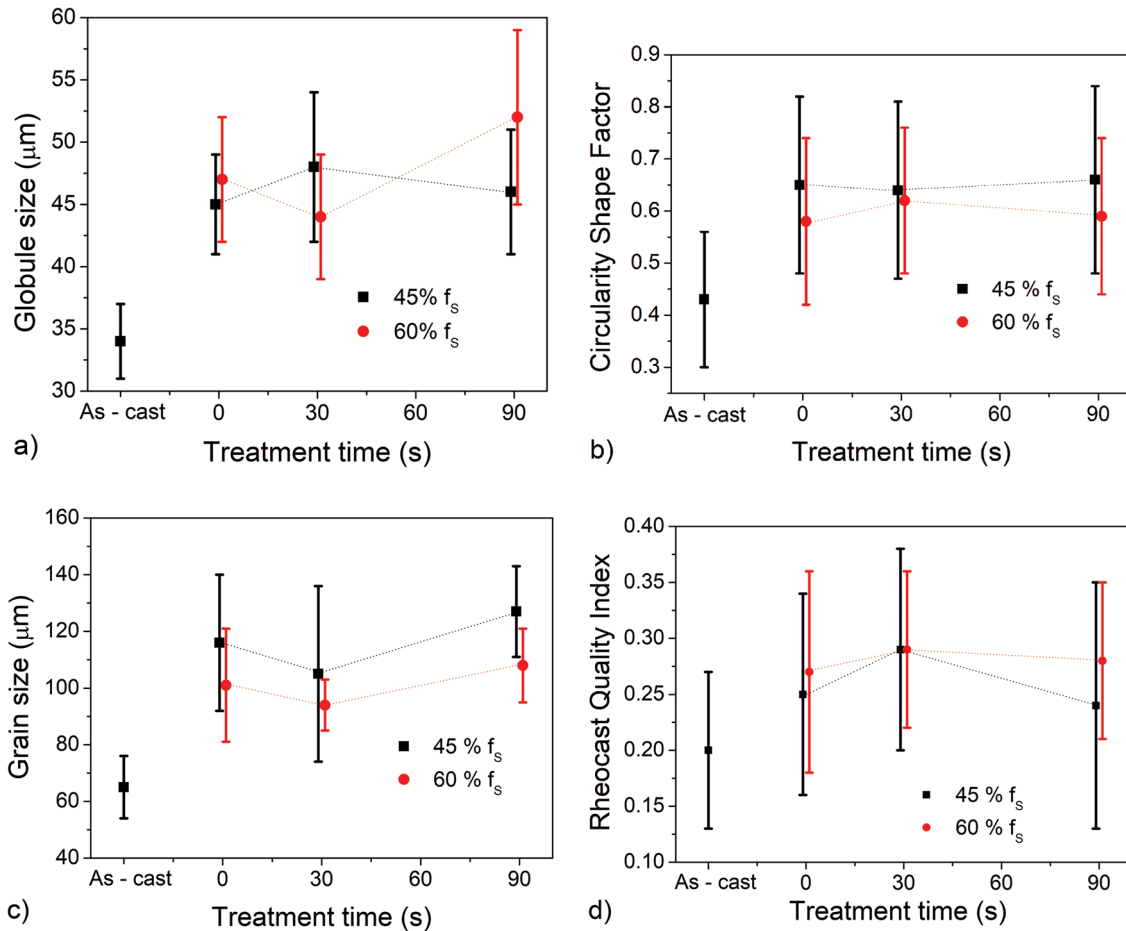


**Fig. 7** Summary of the metallurgical parameters of the heat-treated Al<sub>3</sub>Si<sub>2.5</sub>Cu alloy for the 45% and 60% solid fractions at different treatment times

Note that excellent microstructure stability is achieved after reheating regardless of the solid fraction reached. The combination of thermodynamic and microstructural stability will result in little or no variability in apparent viscosity, ensuring reasonable processing control and good die-filling.

## Conclusion

During the globularization heat treatment, the microstructures of the Al<sub>3</sub>Si<sub>2.5</sub>Cu alloy produced via equal channel angular pressing presented globular morphology since the treatment times of 0 s, in both solid fractions, with the effects of the recrystallization



followed by Ostwald Ripening and coalescence being responsible for such phenomena. Therefore, the use of the ECAP process through a single pass was sufficient to generate a metallic slurry with globular solid particles, achieving an average primary globule size of 47  $\mu\text{m}$ , a circularity of 0.62, an average grain size of 108  $\mu\text{m}$ , and a corresponding Rheocasting Quality Index values around 0.27, showing an excellent refinement of the material structure and consequently proving to be an alternative and effective route for thixoforming processes. In this case, times of 30 s at the semisolid state are enough to ensure the best condition for processing. As thermodynamic and microstructural stability guarantees reasonable viscosity control and good processing control, the raw material production route via ECAP can be an excellent solution for thixoforming processes, especially for these alloys with low silicon content.

**Acknowledgment** The authors would like to thank FAPESP (State of São Paulo Research Foundation—Projects 2009/08478-1, 2015/22143-38, 2018/11802-4 and 2022/05050-5) and CNPq (National Council for Scientific and Technological Development—Project Pq 303299/2021-5) for providing financial support. The authors are also grateful to FEM/UNICAMP (Faculty of Mechanical Engineering, Campinas University) and IFSP (São Paulo Federal Institute of Education, Science and Technology), Bragança Paulista, SP campus.

## References

- M.C. Flemings, Behavior of metal alloys in the semisolid state. *Met. Trans. A*. **22**, 957–981 (1991)
- H.V. Atkinson, Modeling the semisolid processing of metallic alloys. *Prog. Mater. Sci.* **50**, 341–412 (2005)
- Z. Fan, Semisolid metal processing. *Inter. Mat. Reviews*. **47**(2), 49–85 (2002)
- G.S. Cole, A.M. Sherman, Lightweight materials for automotive applications. *Mat. Charact.* **35**(1), 3–9 (1995)
- W.S. Miller, L. Zhuang, J. Bottema, A.J. Wittebrood, P. De Smet, A. Haszler, A. Vieregge, Recent development in aluminium alloys for the automotive industry. *Mat. Sci. Eng. A*. **280**(1), 37–49 (2000)
- E. Schubert, M. Klassen, I. Zerner, C. Walz, G. Sepold, Lightweight structures produced by laser beam joining for future applications in automobile and aerospace industry. *J. Mater. Proc. Tech.* **115**(1), 2–8 (2001)
- EAA, European Aluminium Association. <https://www.european-aluminium.eu/>. Accessed April 2018
- ABAL, Associação Brasileira do Alumínio. <http://www.abal.org.br>. Accessed March 2018
- V.M. Segal, Materials processing by simple shear. *Mat. Sci. Eng. A*. **197**, 157–164 (1995)
- T.J. Chen, G.X. Lu, Y. Ma, Y.D. Li, Y. Hao, Microstructural evolution during partial remelting of equal channel angular pressed ZW21 magnesium alloy. *J. Alloys Comp.* **486**, 124–135 (2009)
- Z. Zhao, Y. Cheng, Q. Chen, Y. Wang, D. Shu, Reheating and thixoforging of ZK60+RE alloy deformed by ECAP. *Trans. Nonfer Met. Soc. China*. **20**, 178–182 (2010)
- S. Ashouri, M. Nili-Ahmadabadi, M. Moradi, M. Iranpour, Semisolid microstructure evolution during reheating of aluminium A356 alloy deformed severely by ECAP. *J. Alloys Comp.* **466**, 67–72 (2008)
- M. Moradi, M. Nili-Ahmadabadi, B. Poorganji, B. Heidarian, M.H. Parsa, T. Furuha, Recrystallization behaviour of ECAPed A356 alloy at semisolid reheating temperature. *Mat. Sci. Eng. A*. **527**, 4113–4121 (2010)
- L.V. Torres, E.J. Zoqui, Microstructural stability and rheological behavior of Al–Si–Cu alloys in the semisolid state. *Met. Mat. Trans. B*. **53**, 3229–3245 (2022)
- D. Liu, H.V. Atkinson, H. Jones, Thermodynamic prediction of thixoformability in alloys based on the Al–Si–Cu and Al–Si–Cu–Mg systems. *Acta Mat.* **53**(14), 3807–3819 (2005)
- L.V. Torres, L.F. Torres, E.J. Zoqui, Electromagnetic stirring versus ECAP: morphological comparison of Al–Si–Cu alloys to make the microstructural refinement for use in SSM processing. *Adv. Mater. Sci. Eng.* **2016**, 9789061 (2016)
- C.T.W. Proni, L.V. Torres, R. Haghayeghi, E.J. Zoqui, ECAP: an alternative route for producing AlSiCu for use in SSM processing. *Mater. Charac.* **118**, 252–262 (2016)
- L.V. Torres, E.J. Zoqui, Metallurgical comparison of Al<sub>2</sub>Si<sub>2.5</sub>Cu and Al<sub>4</sub>Si<sub>2.5</sub>Cu semisolid alloys produced by equal channel angular pressing process. *Matéria*. **25**, e-12628 (2020)
- L.V. Torres, D.M. Benati, E.J. Zoqui, Morphological evolution of Al-2 wt%Si-2/5 wt%Cu alloy produced by EMS and EMS enhanced by ECAP. *Sol. St. Phen.* **217–218**, 105–110 (2015)
- AMERICAN SOCIETY FOR TESTING AND MATERIALS, ASTM, *E112: Standard test methods for determining average grain size* (West Conshohocken, ASTM, 1996)
- E.J. Zoqui, M. Paes, E. Es-Sadiqi, Macro- and microstructure analysis of SSM A356 produced by electromagnetic stirring. *J. Mater. Process. Tech.* **120**, 365–373 (2002)
- K.N. Campo, E.J. Zoqui, Thixoforming of an ECAPed aluminium A356 alloy: microstructure evolution, rheological behavior, and mechanical properties. *Metal. Mater. Trans. A*. **47**, 1792–1802 (2016)

**Publisher's Note** Springer Nature remains neutral with regard to jurisdictional claims in published maps and institutional affiliations.

Springer Nature or its licensor (e.g. a society or other partner) holds exclusive rights to this article under a publishing agreement with the author(s) or other rightsholder(s); author self-archiving of the accepted manuscript version of this article is solely governed by the terms of such publishing agreement and applicable law.